LOW WIRE COUNT LOADS

R. E. Terry* and J. P. Apruzese*

*Radiation Hydrodynamics Branch, Plasma Physics Division Naval Research Laboratory, Washington, DC 20375 USA

Abstract

Energetic implosions, using two or three load wires to create a focused axial stagnation of dense wire cores amidst the assembled precursor plasma, are examined with respect to the trade between the implosion mass lost to precursor ablation and the mass or kinetic energy available at stagnation. The calculated kinetic energy at stagnation serves as measure for the output x-radiation.

I. INTRODUCTION

The use of a single wire load on large machines like "Z" is usually avoided due an excessive initial inductance and subsequent high voltages on upstream components. There is however a middle ground where a few larger wires can start well off axis and present much less initial inductance. Such loads will provide the lower inductance at the expense of more precursor plasma involvement.

In contrast to closed arrays with hundreds of fine wires, this relatively unexplored path to energetic implosions would use two or perhaps three load wires of appropriately heavier mass and aims to create a focused axial collision of dense wire cores amidst the assembled precursor plasma. The precursor, not confined by many wires, would presumably not soften this collision.

Hence we must examine the trade between the implosion mass lost to precursor ablation and the mass available to deliver the wire core's kinetic energy.

A clear consequence of this load choice is a quite open geometry for which the transition to a highly conducting annular MHD plasma is neither an early nor a necessarily dominant feature of the electrodynamics. Generalizing slightly beyond MHD, we use a Lorentz gauge direct field solver to treat the TEM to TM mode set transition in the pinch region. The problem is formulated using a scalar potential Φ and an axial vector potential A_z as unknowns, with the radial vector potential A_r being determined by the gauge constraint.

In contrast to earlier wire dynamic model (WDM) formulations with inductance matrix elements good only in the thin wire limit[1], the present work will make use of a new analytic Green's function for A_z that accounts for proximity effects among the wire cores and the return current structure.

The Green's function provides a first estimate for the axial vector potential solution $A_z(x,y)$ at the pinch midplane and the net load inductance arising among the heavy wire filaments. That solution is further refined by a current density source term representing the extended coronal plasma conductivity and flow.

The use of empirical mass source terms[2], for estimating the precursor mass ejection rate and ablation velocity, is then introduced to complete the picture.

II. MATHEMATICAL FORMULATION

There are two required innovations to get the results we want. First, we must go beyond the thin wire inductance limit, which is fine for wire core dynamics and current sharing, but starts to break down when the tenuous corona plasma jackets the wires and entrains current. Moreover, in the larger wires used for the loads we consider, proximity effects become noticeable as the wires approach one another. Hence a means of describing the extended conduction medium of the corona while maintaining contact with the lowest order inductive picture enforced by the wire cores is key to a versatile picture.

Second, we require a fluid description that admits a large adaptability in scale lengths in order to track the history of coronal plasma elements that drift radially to form the axial precursor. A smooth generalization of the discrete wire filaments into fluid particles allows a large dynamic range in mesh size for the field solver. The new fluid particle methods used here adapt easily to such grids because the projection of the fluid particle variables like density, velocity, and energy onto the Eulerian grid is virtually exact.

Report Documentation Page

Form Approved
OMB No. 0704-0188

1. REPORT DATE	2. REPORT TYPE	3. DATES COVERED
JUN 2003	**N/A**	**-**

4. TITLE AND SUBTITLE	5a. CONTRACT NUMBER
Low Wire Count Loads	5b. GRANT NUMBER
	5c. PROGRAM ELEMENT NUMBER
6. AUTHOR(S)	5d. PROJECT NUMBER
	5e. TASK NUMBER
	5f. WORK UNIT NUMBER
7. PERFORMING ORGANIZATION NAME(S) AND ADDRESS(ES) **Radiation Hydrodynamics Branch, Plasma Physics Division Naval Research Laboratory, Washington, DC 20375 USA**	8. PERFORMING ORGANIZATION REPORT NUMBER
9. SPONSORING/MONITORING AGENCY NAME(S) AND ADDRESS(ES)	10. SPONSOR/MONITOR'S ACRONYM(S)
	11. SPONSOR/MONITOR'S REPORT NUMBER(S)

12. DISTRIBUTION/AVAILABILITY STATEMENT
Approved for public release, distribution unlimited

13. SUPPLEMENTARY NOTES
See also ADM002371. 2013 IEEE Pulsed Power Conference, Digest of Technical Papers 1976-2013, and Abstracts of the 2013 IEEE International Conference on Plasma Science. IEEE International Pulsed Power Conference (19th). Held in San Francisco, CA on 16-21 June 2013. U.S. Government or Federal Purpose Rights License, The original document contains color images.

14. ABSTRACT
Energetic implosions, using two or three load wires to create a focused axial stagnation of dense wire cores amidst the assembled precursor plasma, are examined with respect to the trade between the implosion mass lost to precursor ablation and the mass or kinetic energy available at stagnation. The calculated kinetic energy at stagnation serves as measure for the output x-radiation.

15. SUBJECT TERMS

16. SECURITY CLASSIFICATION OF:			17. LIMITATION OF ABSTRACT	18. NUMBER OF PAGES	19a. NAME OF RESPONSIBLE PERSON
a. REPORT	b. ABSTRACT	c. THIS PAGE			
unclassified	**unclassified**	**unclassified**	**SAR**	**4**	

A. Energy Transfer in a Circuit Model

For the original WDM the direct interaction among an ensemble of current elements is equivalent to a potential energy defined by the array inductance. Within the ensemble are symmetry groups of multiplicity S, e.g.

$$I = \Sigma_{is=1,1}^{N,S} J_{i,s} = I\Sigma_{i=1}^{N} S\alpha_i \ , \tag{1}$$

where α_i is any S-wise invariant current fraction contained in any particular wire path represented by a series resistance and inductance.

By construction then the sum of all α_i is one. Since the wire paths are in parallel, the voltage seen by each path α_i is equal in the absence of (small) wave transit time effects. If we examine the voltage $V_e(t)$ impressed at the entrance or feed of a wire array cage, then from the following figure, the resolution of the set α_i and the total current I admitted to the array are seen to be two distinct problems. From the view of the external generator $V_g(t)$, the array is a two terminal device and the energy into it must be the same for all sets α_i that show the same net impedance.

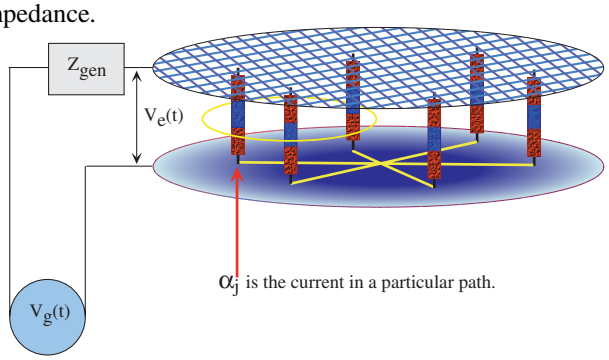

Figure 1. WDM circuit elements can decompose into symmetry groups, with each element representing a resistance and inductance.

Maintaining equal voltage at each circuit element, the equations fixing the current fractions α_i for any given $V_e(t) = V_g(t) - Z_{gen}I$ and I can be written as,

$$V_e(t) = R_i(t)\alpha_i I + \left(\frac{d}{dt}\mathbf{L}_{ij}\cdot\alpha_j I\right) \ , \tag{2}$$

and then integrated over a time interval $\delta \equiv \frac{V_e(t)}{dV_e/dt}$ to eliminate the time derivative. Denote by $\Delta\Psi_e$ the change in flux over this interval, the matrix relation

$$\frac{\Delta\Psi_e}{I}\mathbf{u}_i = \delta R_j \mathbf{I}_{ij}\cdot\alpha_j + \mathbf{L}_{ij}\cdot\alpha_j \tag{3}$$

emerges, with $\mathbf{I}_{ij}$ the diagonal identity matrix, $\mathbf{u}_i$ a unit vector over the local group.

In the limit of vanishing inductance, or slow timescales ($\delta \gg L_i/R_i$), it is easy to see that the $\alpha_i = Z_{||}/R_i(t)$ and thus they clearly add up to unity.

B. Field Methods for Open Geometries

Loads with fewer wires using larger initial wire diameters and load radii will present a lower initial inductance at the expense of more precursor plasma involvement. In contrast to closed arrays with hundreds of fine wires, this very open field geometry is positioned on the edge of validity for a conventional inductance and MHD picture due to the large dynamic range in scale lengths and magnetic Reynolds number. The limit of spatially constant voltage throughout the corona is probably pretty good but by no means certain.

1. Mode Transitions from TEM to TM

With $Z_o = \sqrt{\varepsilon_o/\mu_o} = 367.7\Omega$, an inlet TEM boundary condition on the scalar potential $\Phi(r,z,t)$

$$V_{in} = Z_L I_c = \left[\frac{Z_o}{2\pi}\ln(\frac{r_>}{r_<})\right] I_c \ , \tag{4}$$

determines all the fields near the inlet, where $\mathbf{A} \to 0$.

Elsewhere, the time integral of the scalar potential forms a useful generalization of the familiar inductive "flux function", viz. let $\Psi(r,z,t) = \int^t dt_1 \Phi(r,z,t_1)$, and

$$\Psi(r_>) - \Psi(r_<) = \int_{r_<}^{r_>} \mathbf{A}_r(z_c, r_1, t)dr_1 \ , \tag{5}$$

$$\Psi(z_>) - \Psi(z_<) = \int_{z_<}^{z_>} \mathbf{A}_z(z_1, r_c, t)dz_1 \ , \tag{6}$$

on radial z_c and axial r_c conductor boundaries to ensure that the tangential component of electric field vanishes.

2. Utility of the Lorentz Gauge

The Lorentz gauge condition choice

$$r^{-1}\partial_r(r\mathbf{A}_r) + \partial_z\mathbf{A}_z + c^{-2}\partial_t\Phi \equiv 0 \ , \tag{7}$$

allows the dynamics to concentrate on the solution of $\mathbf{A}_z(z,r,t)$ only. One may in fact examine only two coupled wave equations for the needed fields.

$$\nabla^2\Phi - c^{-2}\partial_t^2\Phi = 0, \tag{8}$$

$$\nabla^2\mathbf{A}_z - c^{-2}\partial_t^2\mathbf{A}_z = -\mu_o\mathbf{J}_z, \tag{9}$$

with the axial current density near the wires given by

$$\mathbf{J}_z = \sigma_\perp\left[\mathbf{E}_z + \mathbf{V}_r\times\mathbf{B}_\theta(\mathbf{A})\right] \ . \tag{10}$$

For the inhomogeneous wave equation involving $\mathbf{A}_z(x,y)$, a Green's function can be developed for the

problem at the diode mid-plane which captures the proper boundary conditions on the outer return current surface and on the finite size conducting wire cores. The function can be built up piecewise from image currents generated by a source cylinder (a), any number of floating cylinders b,b',... and the return cylinder (c),

$$\mathscr{G}(x,y|s=a,b,b'\ldots) = g_a(x,y)+g_b(x,y)+$$
$$g_{b'}(x,y)+g_{xb}(x,y)+g_{xb'}(x,y)+\ldots\,, \qquad (11)$$

and over the symmetry groups $\mathbf{A}_z(x,y) = \Sigma_s \mathscr{G}(x,y|s)$. This $\mathbf{A}_z$ "diagonalizes" the inductance matrix.

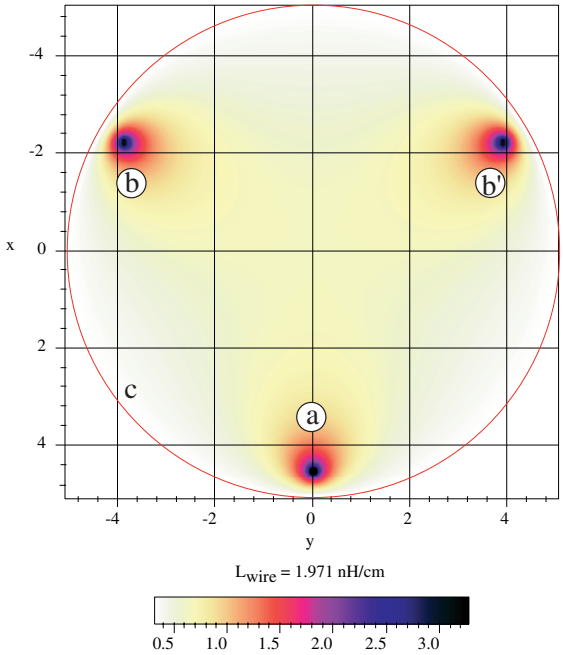

Figure 2. Three 1000 μm Wire Vector Potential $A_Z(x,y)$

3. Variational Form of the Field Problem

Dimensionless spatial variables are based on a characteristic time t_o of the input pulse line, $\lambda_o = ct_o$, and a skin depth $\delta_o = \sqrt{\frac{2t_o}{\mu_o\sigma_\perp}}$.

With $\mathscr{E}_z = t_o \mathbf{E}'_z$, action integrals advance all fields,

$$\mathscr{L}(\Phi) = \int d\tau dA \left[(\nabla\Phi)^2 - (\partial_\tau\Phi)^2\right]\,, \qquad (12)$$

$$\mathscr{L}(\mathbf{A}_z) = \int d\tau dA \left[(\nabla\mathbf{A}_z)^2 - (\partial_\tau\mathbf{A}_z)^2 - \mathbf{A}_z(\frac{2\lambda_o}{\delta_o})^2\mathscr{E}_z\right]\,. \qquad (13)$$

Our finite element (FE) representation employs value and time derivative degrees of freedom, e.g. $\vec{\Phi} = [\Phi, \partial_\tau\Phi]$. The variation

$${}_{i+1}\mathbf{W}_{i+1}\cdot{}^{i+1}\vec{\Phi} + {}_{i+1}\mathbf{W}_i\cdot{}^{i}\vec{\Phi} + {}_{i+1}\mathbf{W}_{i-1}\cdot{}^{i-1}\vec{\Phi} \equiv 0\,, \qquad (14)$$

is equivalent to solving the PDE problem. The symmetric positive definite weight matrices have the general form, ${}_l\mathbf{W}_m = T_{lm}\otimes(G_x+G_y) - T'_{lm}\otimes V$ with integrals of squared time values T, time derivatives T', spatial gradients G, and spatial values V taken over each cell.

C. Particle Methods

The original formulation[3] used freely drifting particles only and focused on particle annihilation and creation rules to track emerging features.

The novel particle solutions used here are drift kinetic fluid particles (DKFP) and track precisely the distribution function evolving under the action of the drift velocity $\mathbf{C}$ and acceleration $\mathbf{A}$ which are functions of local position $\mathbf{x}$, $\mathbf{C} = \mathbf{V} + \mathbf{x}\cdot\delta/h$, $\mathbf{a} = \mathbf{A} + \mathbf{x}\cdot\alpha/h$.

These DKFP contain three common factors which represent the dilation of the initial size (due to the shear in the velocity and acceleration), and the (asymmetric) movement of the initial domain boundaries. For a 1D particle class these are:

$$D(t) = (1 + \frac{t\,\delta}{h} + \frac{1}{2}\frac{t^2\alpha}{h})\,, \qquad (15)$$

$$h_\pm(t) = \pm h + (V \pm\pm\delta)\,t + \frac{1}{2}(A\pm\pm\alpha)\,t^2\,. \qquad (16)$$

The expected profile for number density (per unit length, area, or volume) $n(X,t) \equiv < N > /\ell$ is then:

$$n(X,t) = \frac{N}{2hD(t)}\left(\mathrm{erf}\left(\frac{(h_+(t)-X)}{\sqrt{2}Ut}\right) + \mathrm{erf}\left(\frac{(X-h_-(t))}{\sqrt{2}Ut}\right)\right)\,, \qquad (17)$$

with similar expressions for momentum and enthalpy. The fluid properties, needed by the electrodynamics to support the evaluation of a magnetic Reynolds number ($\mathscr{R}_m = 2\ell_B t_o V_r/\delta_o^2$) and the source term above, are then easily projected into each node or cell of the field solution grid with virtually no error.

1. Source Boundary Conditions at the Wire Core

The detailed accounting of material phase changes as the wires vaporize and ionize is left to future refinements. A reasonably simple and apparently accurate approximation is to balance the force of the wire core attraction with a "rocket" force due to the inward flow of coronal plasma[2]. Here a strict balance is too specialized, for what is needed is a path to account for wire loads that do not hang at the initial radius until they virtually disintegrate. From earlier work[4] we know that Al foil switches exhibit an areal mass loss rate that scales directly with the surface magnetic energy density, viz. $\partial_t m = -\kappa\frac{B^2}{8\pi}$,

and a flow velocity determined by a sound speed[5] or, as seen for switch foils, an Alfven speed characterized by local field or "private flux" near the wire. Such considerations lead to a mass loss estimate, for a wire of length ℓ and radius r_{wire}, that scales like

$$\dot{m} \approx 10\kappa(\ell/r_{wire})I^2_{[MA]}[\mu g/ns] \ . \qquad (18)$$

Typical values for κ are [5-25] $\mu gcm/ergs$ and we find that, in keeping with the other models cited here, only a small fraction of the wire current ($\approx 10^{-2}$) can be viewed as directly participating in this erosion process. The larger current fraction must be concentrated outside the core in the vapor and plasma emitted by the wire.

2. Magnetoplasma Conductivity

The Epperlein-Haines[6] formulation for the required skin depth δ_o in the wire corona can be written

$$1/\sigma_\perp \equiv \eta_\perp = \eta_0 \ \alpha_\perp(Z, \omega\tau) \qquad (19)$$

with, $\alpha_\perp(Z, \omega\tau)$ a rational function, and

$$\eta_0 \equiv \left[\frac{m_e}{e^2 n_e \tau_e}\right] \ = 1.147519 \cdot 10^{-14} \ \frac{Z \ln\Lambda}{T^{3/2}_{[eV]}} \ [s]. \qquad (20)$$

As needed in the $\mathbf{A}_z$ source term, for a time t_o,

$$(\frac{\lambda_o}{\delta_o})^2 = 1.218472 \cdot 10^{-2} \ \frac{\lambda_o^2}{2t_o} \frac{T^{3/2}_{[eV]}}{\ln\Lambda \ Z \ \alpha_\perp(Z, \omega\tau)} \qquad (21)$$

is the (dimensionless) equivalent.

III. EARLY INDUCTANCE AND ENERGY AT STAGNATION

First we have examined the question of initial inductances for loads that might be contemplated on larger machines like "Z". For 1,2, and 3 wire loads set at 0.9 of the return current radius, one sees quite favorable inductances for diameters near or above 100μm. The larger masses shown in Table 1 above 100μm clearly would not be viable, but here hollow loads of large radius and lower mass should be examined.

Table 1. Initial Inductances and Masses for Ti Loads

Size μm	L_1 $\frac{nH}{cm}$	L_2 $\frac{nH}{cm}$	L_3 $\frac{nH}{cm}$	Mass $\frac{\mu g}{cm}$
1000	5.88	2.95	1.97	...
500	7.27	3.64	2.43	...
200	9.11	4.56	3.05	1,426
100	10.49	5.25	3.51	357
50	11.98	5.95	3.97	89.2
20	13.71	6.86	4.58	14.26
10	15.10	7.55	5.04	3.57

With a load mass m_i in μgm per wire, inductance L in nH, driver voltage V in MV, and pinch dimensions of length ℓ, and radius r_0 in cm, the available wire core energy at stagnation scales as,

$$K_{imp,2} = 522.4 \left(r_0 \ (m_i\ell)^{1/2} \ V/L\right) \ [kJ]. \qquad (22)$$

One expects, $K_{imp,3} = \sqrt{4/3}K_{imp,2}$ for the three wires.

We have (i) modified the wire dynamic model (WDM) to the calculation of kinetic energy transfer to such low wire number loads on both Double Eagle and "Z" class drivers. and (ii) assessed the load energy and upstream voltages.

For DE any initial mounting of two or three 50 to 200 μm Ti wire loads at radii in excess of 0.6 of the return current radius will easily preclude early voltages near the insulator stack from rising above one half the open circuit voltage as the load initiates and starts to run in. The best available kinetic energies are about 80 kJ for two wire loads, and about 100 kJ for three wire loads. The (60-80 μg/cm) masses required are typical for DE, the inductive current "bite" is clear.

For "Z" again initial mounting of similar wire loads at radii in excess of 0.6 of the return current radius will also keep early voltages in bounds. The best available kinetic energies are about 600 kJ for two wire loads, and about 900 kJ for three wire loads. The (250-375 μg/cm) masses used are an excellent match in "Z".

In both cases the result of too much mass erosion is to degrade the available kinetic energy at stagnation.

Acknowledgements

The authors wish to acknowledge discussions with A. Velikovich and M. Haines. Maple software was instrumental in this research, which was sponsored by DTRA.

REFERENCES

1. R. E. Terry, *et al*, PRL, **83**(21), 1999.
2. S. V. Lebedev, *et al*, Phys.Plasmas, **8**(8), 3744(2001).
3. Bateson and Hewett, JCP **144**, 358-378(1998).
4. J. E. Brandenburg, R. E. Terry, N. R. Pereira, "Mass Erosion in Foil Switches",*Fourth Int'l Conf on Megagauss Fields*, Plenum Press, New York, 1986, p.543.
5. M. G. Haines, Phys.Plasmas, **30**(2), 588(2002).
6. E. M. Epperlein and M. G. Haines, Phys. Fluids, **29**(4), 1986.